Atmospheric Research, 30 (1993) 157–170
Elsevier Science Publishers B.V., Amsterdam

Sensitivity of monsoon rainfall predictions to initialization procedures

K. Alapaty[a], R.V. Madala[b] and S. Raman[a]

[a]*Department of Marine, Earth and Atmospheric Sciences, North Carolina State University, Raleigh, NC 27695, USA*

[b]*Naval Research Laboratory, Washington, D.C. 20375, USA*

(Received November 2, 1992; revised and accepted March 18, 1993)

ABSTRACT

Prediction of orographic-convective rainfall during an active monsoon period is studied with an adiabatic and a diabatic vertical mode initialization schemes. A nested grid mesoscale model is used to perform two numerical simulations. In the diabatic initialization scheme, vertical distribution of latent heat released in convective clouds is obtained using the Kuo scheme from analyzed rainfall rates. Results indicate that the model predicted significantly higher rainfall rates when the initial conditions are obtained using a diabatic initialization scheme. Also, predicted rainfall rates are persistently higher almost throughout the period of simulation with a considerable increase during the first nine hours of integration when initial conditions are obtained from a diabatic initialization scheme. Use of diabatic initialization scheme lead to the prediction of stronger winds, stronger circulation patterns associated with the cumulus convection and higher latent heat fluxes from surrounding oceans, leading to higher rainfall rates.

RÉSUMÉ

On étudie la prévision de précipitation orographique convective pendant une période active de mousson à l'aide de schémas avec initialisation en mode vertical adiabatique et diabatique. On utilise un modèle de mésoéchelle à grilles emboitées afin de réaliser deux simulations numériques. Dans le schéma à initialisation diabatique, la distribution verticale de la chaleur latente libérée dans les nuages convectifs est obtenue à l'aide du schéma de Kuo à partir de l'analyse des taux de précipitation. Les résultats montrent que le modèle prédit des taux de précipitation nettement plus élevés lorsque les conditions initiales sont obtenues par un schéma d'initialisation diabatique. De plus, dans ce cas, les taux prévus de précipitation sont plus élevés pendant pratiquement toute la période de simulation, avec une augmentation considérable dans les neuf premières heures d'intégration. L'utilisation d'un tel schéma conduit à la prévision de vents plus rapides, d'une circulation plus forte associée à la convection nuageuse et d'un flux de chaleur latente plus élevé à partir des océans, le tout conduisant à des taux de précipitation plus forts.

INTRODUCTION

Short range prediction of rainfall in the regional and global scale models is mainly affected by the inaccuracies in the input data namely, the divergence,

moisture and the mass fields. A numerical study of the effect of initial moisture analysis on the rainfall predictions (Wolcott and Warner, 1981) indicates that the most realistic amounts of rainfall are produced when a saturation constraint was imposed by the use of satellite and surface-based observations. Also, it was found (Wolcott and Warner, 1981) that the cumulus convection in the model sustains only in the presence of proper convergence field in the initialized initial conditions. Using a general circulation model, Mohanty et al. (1986) studied the impact of diabatic heating on the initialization of divergent circulations in the tropics. They also found that the initial large-scale divergent circulations were not retained during the forecast period unless the model was forced to generate a diabatic heating sufficiently similar to the observed heating. Puri (1987) studied the use of tropical diabatic heating information for initial state specification and found that the persistence of dynamical balance during model integrations is strongly dependent on the compatibility between the specified heating during initialization and the heating during the model integration. One of the shortcomings in these studies is the a priori assumption of the magnitude and the vertical distribution of heating rates used in the diabatic initialization schemes. To alleviate this problem, satellite-based data such as infrared and visible imagery data (Turpeinen et al., 1990) or outgoing longwave radiation data (Puri and Miller, 1990) are used to estimate the initial convective heating rates for use in the initialization schemes.

During the monsoon season, the westcoast of India is one of the regions where large rainfall rates are observed. Analyzed rainfall data for the monsoon region (Krishnamurti et al., 1983) indicate maximum rates of about 200 mm d^{-1} along the westcoast of India. Though there exists some uncertainty in the analyzed rainfall rates, (pers. commun. with T.N. Krishnamurti), these provide an unique opportunity to study the effects of initialization procedures on a model forecast. The objective of this paper is to study the effects of diabatic and adiabatic initialization procedures on the monsoon rainfall prediction using a nested grid mesoscale model.

THE MODEL

A nested grid model developed at the Naval Research Laboratory and North Carolina State University is used for numerical simulations. It is a primitive equation model written in pressure-based terrain-following σ-coordinate system having a one-way interacting nested grid network. Physics included in the model are for convective and nonconvective precipitation, and atmospheric boundary layer processes. Atmospheric radiation is not considered because of the relatively short model integration time (48 h). Convective precipitation is parameterized using modified Kuo scheme (Kuo, 1974; Anthes, 1977). Nonconvective precipitation occurs in the model when super satura-

tion is reached on the resolvable scale. Excess moisture precipitates into lower model layers and evaporates or falls to the surface. A dry convective adjustment scheme, which conserves total static energy, is included in the model above the atmospheric boundary layer to remove superadiabatic lapse rates. There are ten uniform vertical levels in the model and the lowest layer represent the boundary layer. For the horizontal differencing, a staggered grid network (Arakawa C-grid) is used with p_s, q, T, ϕ, and $\dot{\sigma}$ specified at the same horizontal points, and u and v are interlaced between them, where p_s is the surface pressure, q the specific humidity, T the temperature, ϕ the geopotential, $\dot{\sigma}$ the vertical velocity, u the zonal wind and v the meridional wind. Horizontal grid resolutions in the coarse-grid mesh (CGM) and the fine-grid mesh (FGM) domains are 1.5° and 0.5°, respectively. Figure 1 shows the simulation domain for the CGM and the FGM. The CGM domain covers from 37.5° E to 112.5° E and 20.5° S to 42.5° N and the FGM domain from 56.5° E to 100.0° E and 3.0° S to 28.5° N. Envelop topography was obtained from the navy 10′ global topography data for 1.5° and 0.5° horizontal resolutions. Model sea surface temperatures (SST) were obtained from the 1° resolution global climatological values based on a 10 year average for the month of July. Davies scheme (1976, 1983) is employed to provide lateral boundary conditions. At the model top and bottom, the boundary condition for $\dot{\sigma}$ is assumed zero. A split-explicit method is used for the model integrations with

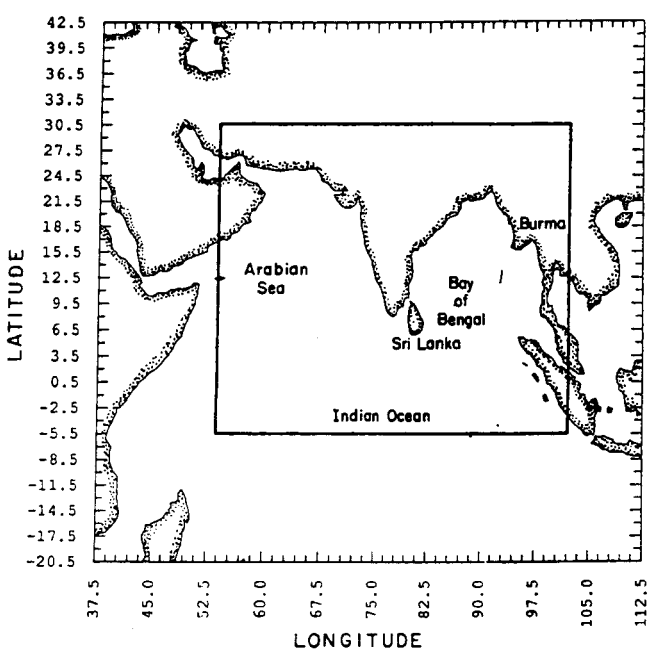

Fig. 1. Model domain of simulation in the coarse grid mesh and the fine grid mesh.

time steps of 300 s and 100 s, in the coarse-grid mesh and the fine-grid mesh domains, respectively. The First GARP Global Experiment (FGGE) level III A data is used to specify the initial conditions.

INITIALIZATION PROCEDURE

An adiabatic vertical mode initialization (AVMI) scheme developed at the Naval Research Laboratory was used to develop a diabatic version (DVMI) of the scheme. To incorporate the latent heat forcing into the AVMI scheme,

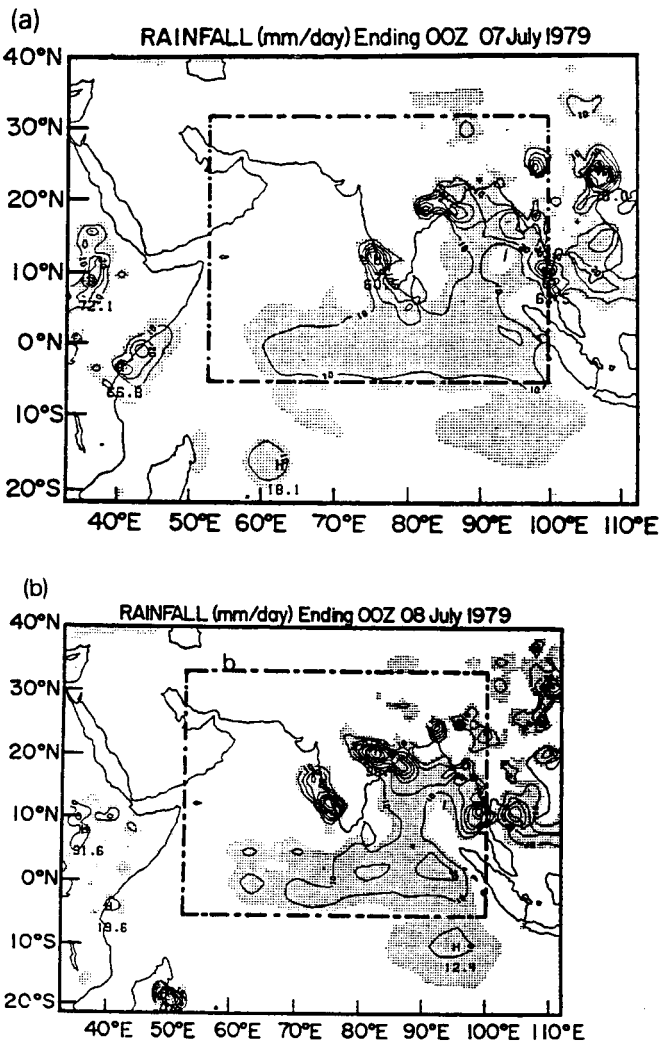

Fig. 2. Analyzed accumulated rainfall distribution by Krishnamurti et al. (1983) for the days (a) 7 and (b) 8 July 1979. Rainfall maximum is located offshore of westcoast of India.

a reverse Kuo scheme was used. Figure 2a and b shows the analyzed accumulated rainfall distribution (Krishnamurti et al., 1983) ending at 00 UTC 7 and 8 July 1979, respectively, for the simulation domain. Dashed box indicates the nested domain. Rainfall rates over the land were obtained from more than 3000 rain gages using a successive correction objective analysis procedure. Rainfall rates over the oceanic region were estimated from the satellite brightness. Though the analyzed rainfall rates over the oceanic region are subject to uncertainties, seaward increase of rainfall indicates that the maximum rainfall associated with the Western Ghats during this period was located just offshore. Rainfall over the Bay of Bengal and eastern India was due to the monsoon depression. Since the rainfall received over the simulation domain was almost due to the cumulus convection, large scale rainfall is thus negligible. Since hourly rainfall rates are not readily available, it is assumed that the previous day of the starting time of simulation has a constant rate of rainfall throughout that day. This constant rainfall rate is converted into convective heating using the reverse Kuo scheme for use in the diabatic initialization scheme. Further, model produced convective heating rates and rainfall for the first three hours of simulation are merged with the corresponding rates from the diabatic initialization scheme. A nonlinear weighting factor (α) is employed where $\alpha=1$ at $t=0$ and $\alpha=0$ at $t=3$ h. The relation is given by:

$$R_m=\alpha R_i+(1-\alpha)R_c \tag{1}$$

where R_i is the convective rainfall rate used in the DVMI, R_c the model-produced convective rainfall rate, R_m the merged rain rate, and α is given by:

$$\alpha=1-[1+\sin(\pi t/3)-(\pi/2)]/2 \tag{2}$$

The above relations allow the influence of the initialized heating and rain rates to approach to zero in a smooth manner. This procedure is done only for the diabatic initialization case.

SYNOPTIC CONDITIONS AND NUMERICAL EXPERIMENTS

During the simulation period (00 UTC 6 to 00 UTC 8 July 1979), monsoon was active and the winds were steady along the westcoast of India. Western Ghats, the mountain range is located about 100 km inland from the westcoast of India. Low level winds approached the westcoast of India almost perpendicular to the Western Ghats. Orographically lifted air generally triggers convective instability over this region, leading to large rainfall rates. A monsoon depression was located over the Burma Coast at 00 UTC 6 July 1979 and moved westward during the next 48 h.

Two numerical simulations are performed for 48 h starting at 00 UTC 6 July 1979. In the first experiment, initial conditions are balanced using the

adiabatic vertical mode initialization scheme while in the second experiment the diabatic vertical mode initialization scheme is used. The coastline in the simulation domain is determined by the model topography data. Thick and bold contours with bold zeros in all plots represent the coastline. Since the coarse-grid model is primarily used to capture the large scale circulations associated with the monsoon flow and also to provide the boundary conditions for the fine-grid model, we present only the results obtained from the fine-grid model simulations. Since the horizontal resolution of the FGGE data is too coarse (2.5°), the monsoon depression can not be represented adequately. The analyzed wind speeds, vorticity and divergence associated with the monsoon depression are very weak in the initial conditions.

RESULTS AND DISCUSSION

Model-predicted rainfall using adiabatic and diabatic VMI schemes are compared with the observations. We refer the results obtained using the adiabatic VMI scheme to as AB case and those obtained using the diabatic VMI to as DB case. As mentioned before, because of some uncertainty in the analyzed rainfall maxima, only spatial distribution of the predicted rainfall is compared with the observations.

Comparison of rainfall rates

Figure 3a and b shows the predicted accumulated rainfall at the end of the first day of simulation (ending at 00 UTC 7 July) for the AB case and the DB case, respectively. It can be noticed that predicted rainfall in both the cases are somewhat similar. For the DB case, areal coverage of predicted rainfall is larger with higher rainfall maximum than that for the AB case. Predicted maximum in both cases exists offshore of the west cost of India with a rate of 74 and 107 mm d^{-1}, for the AB case and DB case, respectively. Comparing with the observations (Fig. 2a), the predicted offshore rainfall maximum seems to be higher for both cases and spatial distribution is somewhat similar. As mentioned earlier, estimated rainfall rates over the oceans are subject to errors, only spatial distribution of observed rainfall is compared with the model predictions rather than the reported maximum rates. Predicted rainfall distribution due to the model's monsoon depression (off the Burma coast) and over the Bay of Bengal in the DB case compares better with the observations (Fig. 2a) than with that for the AB case. In both the AB and DB cases, model does not predict rainfall northeast of India (closer to the eastcoast) while observations indicate a rainfall rate of 50 mm d^{-1}. Predicted circulation patterns associated with the predicted monsoon depression indicated horizontal convergence but cumulus convection did not sustain because of the advection of relatively drier air from the north. Also, vertical cross sec-

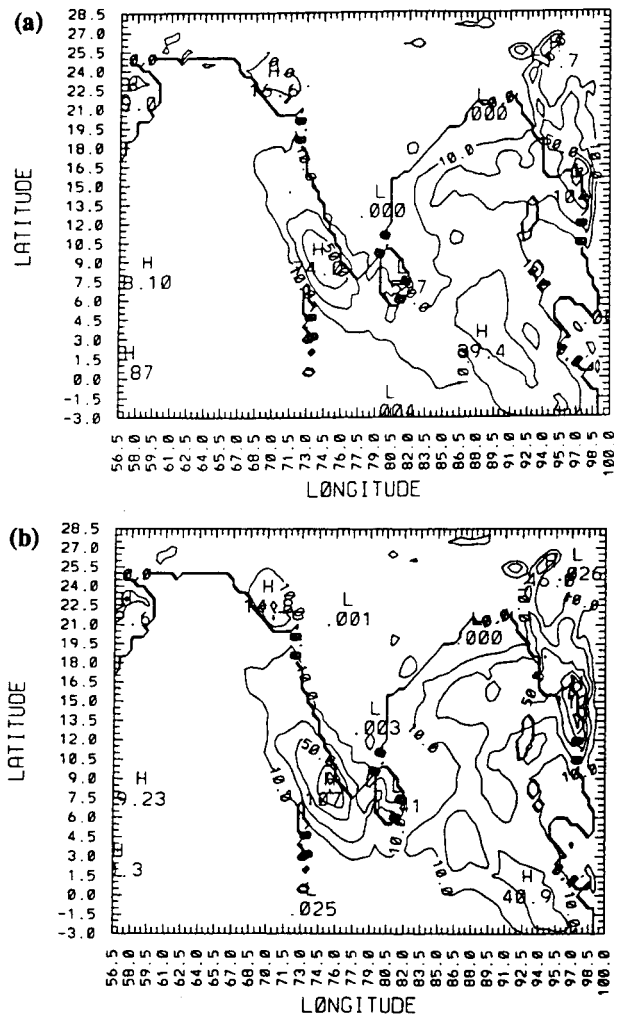

Fig. 3. Predicted rainfall for a period of 24 h ending 00 UTC 7 July (a) in the AB case and (b) in the DB case, respectively. Contour intervals are 10, 25, 50, 75, 100, 125 mm d^{-1}.

tions of the relative humidity at different times during the model integration (not shown) indicated low values, particularly over the northern Indian subcontinent. Uncertainties in the moisture filed in the analyzed FGGE data lead to the poor prediction of rainfall associated with the monsoon depression.

Predicted rainfall rates for the second day of simulation for the AB case and the DB case are shown in Fig. 4a and b, respectively. Predicted rainfall over the oceanic regions is higher in the DB case than in the AB case. Again, predicted rainfall offshore of westcoast of India is higher in the DB case (187

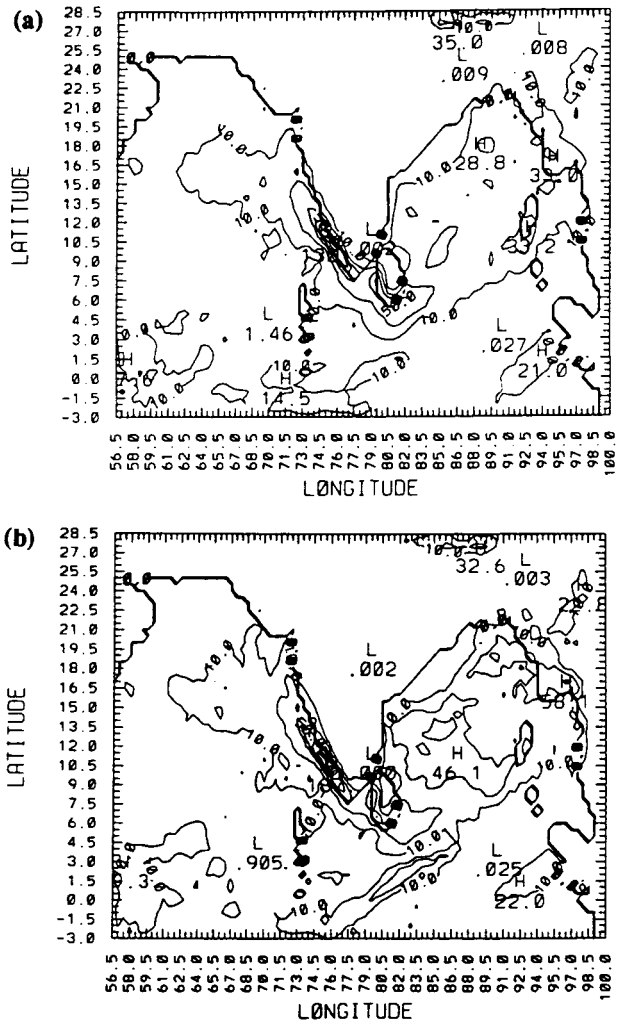

Fig. 4. Predicted rainfall for a period of 24 h ending 00 UTC 8 July (a) in the AB case and (b) in the DB case, respectively. Contour intervals are 10, 25, 50, 75, 100, 125, 150, 175, 200 mm d^{-1}.

mm d^{-1}) than that predicted in the AB case (130 mm d^{-1}) while spatial distribution is similar. Also, comparing with the observed rainfall (Fig. 2b) both the AB and DB cases predict higher rainfall rates and spatial distribution of rainfall in both cases is somewhat comparable to that in the observations. Again, similar to the previous day, in both cases the model did not predict rainfall over the land (over foot hills of Western Ghats closer to the westcoast, northeast India closer to the east coast) and is due to the presence of drier

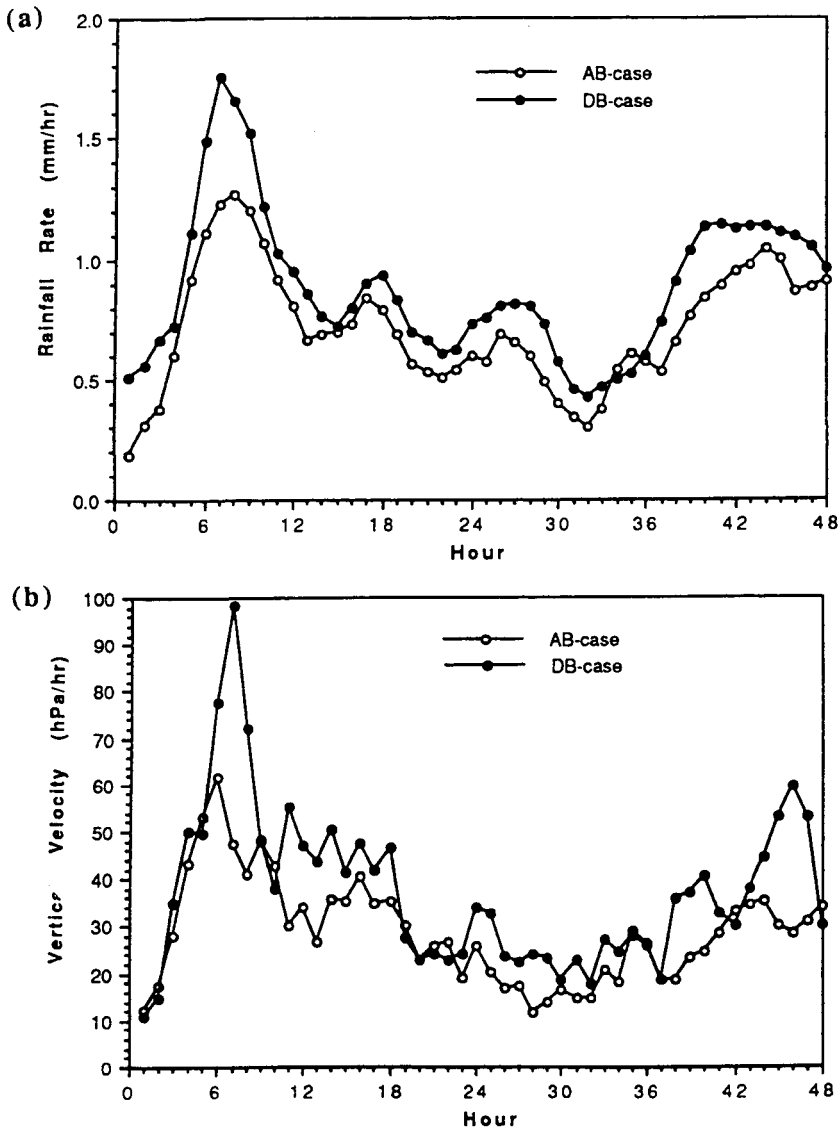

Fig. 5. Temporal variation of (a) area averaged convective rainfall for the area between 6° to 20° N and 70.5° to 76.5° E in the AB case and the DB case, respectively, and (b) domain maximum vertical velocity (ω) for the region 6° to 20° N and 70.5° to 76.5° E at the end of each hour of simulation.

layers. Essentially, predicted rainfall rates are higher for the DB case for both days of simulation, indicating the influence of the diabatic initialization procedure.

To further investigate the effects of the diabatic initialization on the model forecast, area average of accumulated convective rainfall for an area between 6° to 20° N and 70.5° to 76.5° E covering most of the rainfall region near the Western Ghats is considered. Figure 5a shows the temporal variation of area averaged accumulated convective rainfall for the AB case (circles) and for the DB case (dots). During the first nine hours of simulation, predicted area averaged rainfall rates are much higher for the DB case than those in the AB case. This result is due to the enhanced convergence in the lower layers in the DB case where initial conditions are obtained using the diabatic VMI scheme. Also, in the DB case area averaged rainfall is almost persistently higher compared to that in the AB case. This indicates the improvement of model predictions in the DB case where diabatic initialization is used. Signature of the model spinup can be clearly seen in the Fig. 5a where predicted convective rainfall peaks to a maximum at about seven hours starting from the initial time. Also, spinup time required by the model is almost the same for both the simulations. These results are consistent with the results found in other studies mentioned earlier. Also, Turpeinen et al. (1990) found that the diabatic initialization had little impact on the reduction of the spinup time unless the humidity field in the initial conditions was enhanced. Puri and Miller (1990) used the Betts–Miller scheme and rainfall rates derived from the OLR data to initialize the initial moisture field and their results also indicated that reduction in the spinup time occurred only when diabatic initialization and moisture adjustments are performed together.

Figure 5b shows the temporal variation of domain maximum vertical velocity (minimum ω velocity) with in the region considered above for the AB and DB cases. Some noise is present since only instantaneous values of vertical velocities are considered. The vertical velocity field also shows similar behavior to that in the rainfall shown in the Fig. 5a, indicating the presence of model spinup during the early hours of numerical integration. This result also supports the argument (Puri and Miller, 1990; Turpeinen et al., 1990) that diabatic initialization may help in increasing the predicted rainfall rates with no reduction of the spinup time associated with the model.

Comparison of surface moisture fluxes and winds

As mentioned before, the predicted area averaged rainfall and domain maximum vertical velocities for the DB case are almost persistently higher than those in the AB case. Particularly, during the first twelve hours of simulation these are considerably higher. These results indicate that the amount of moisture available for precipitation in the DB case seems to be higher than that in the AB case. To confirm this, accumulated evaporation from the oceans for each day of simulation are considered. Figure 6a and b shows the spatial distribution of latent heat fluxes (averaged for 24 h) for the AB case and the

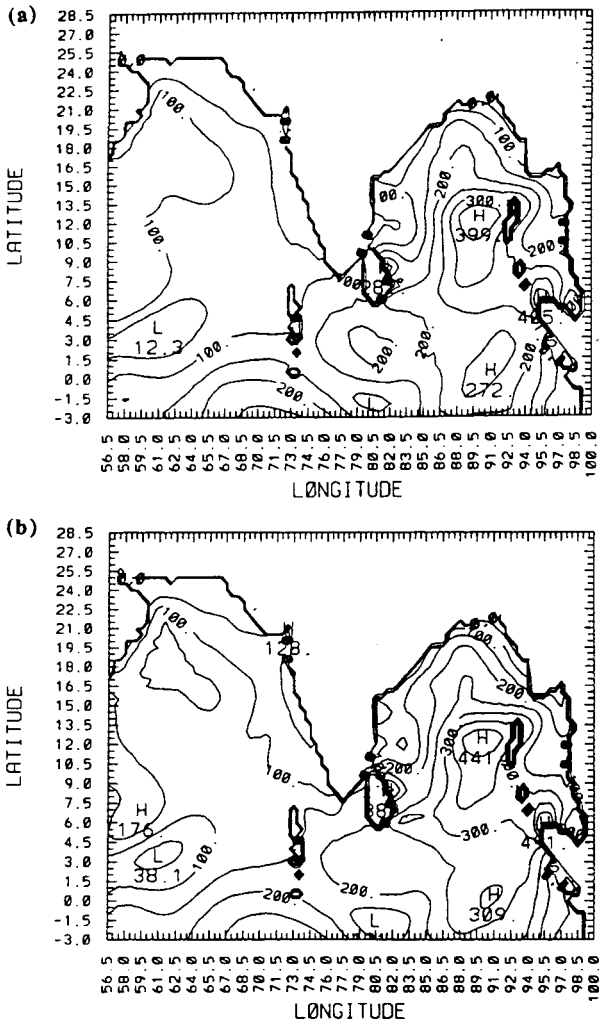

Fig. 6. Spatial distribution of predicted latent heat fluxes at the end of 24 h of simulation (a) in the AB case and (b) in the DB case, respectively. Contour interval is 50 W m^{-2}.

DB case, respectively for the first day of simulation. Increase in the latent heat fluxes over the central Arabian sea, Indian Ocean and the central Bay of Bengal can be noticed. In general, there is an increase in latent heat fluxes of about 40 W m^{-2} can be seen over these regions.

In the diabatic initialization scheme, analyzed rainfall rates are used in estimating the convective heating rates and its vertical distributions. To that effect an additional term is added in the system of equations where calculation of the divergence is of primary interest. As one would expect, the spatial

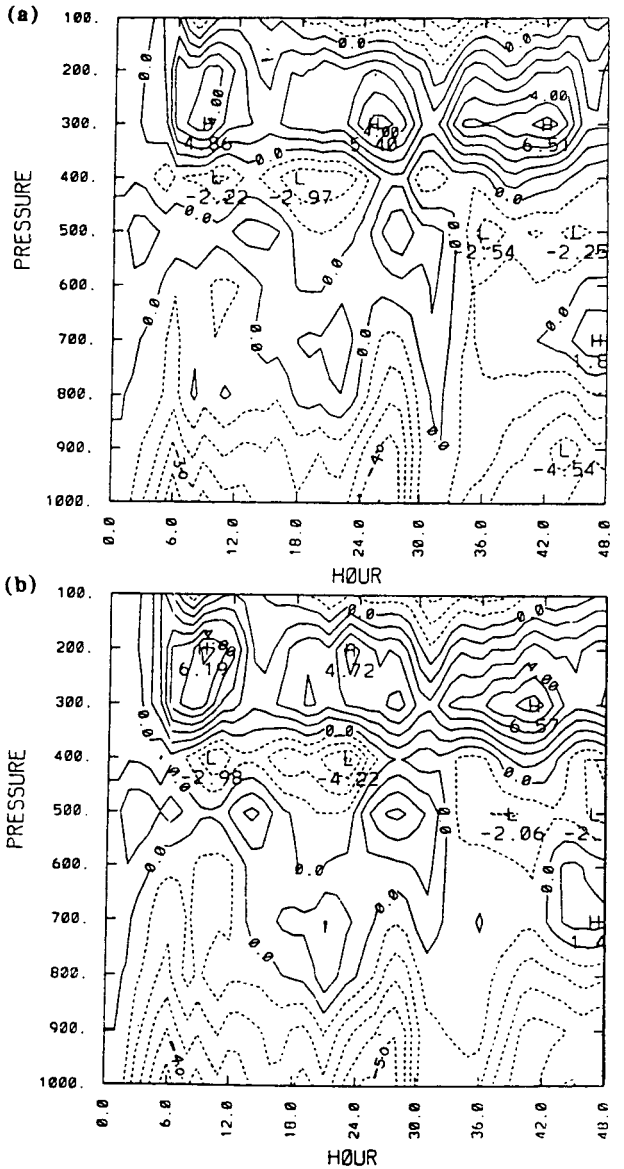

Fig. 7. The height–time section of area averaged divergence for the area between 6° to 20° N and 70.5° to 76.5° E (a) in the AB case and (b) in the DB case, respectively. Contour interval is 1.0×10^{-4} h^{-1}.

distribution of the wind field in the initial conditions for the DB case is different than that for the AB case. Increased convergence in the lower layers (and corresponding increase in the divergence in the upper layers) over the regions of observed rainfall caused local accelerations of the wind for the DB case. The presence of persistently stronger winds over these regions in the DB case lead to the increase in the evaporation from the oceans. Spatial distri-

bution of winds over the Bay of Bengal and Arabian sea for the convectively active regions in the DB case are slightly stronger (about 1.5 m s^{-1}) than those in the AB case during the period of simulation. The differences in the wind fields lead to the differences in the latent heat fluxes. Vertical velocities in the DB case are higher than in the AB case and also larger areal coverage of vertical velocities in the DB case is consistent with the areal increase in the predicted rainfall shown in Fig. 3b. Comparison of these fields for the second day of simulation also indicate somewhat similar results, in agreement with differences in the predicted rainfall in the AB and the DB cases.

Further, to compare differences in the circulation patterns time–height sections of the area averaged (between 6° to 20° N and 70.5° to 76.5° E) divergence field for the AB case and the DB case, respectively are considered and are shown in the Fig. 7a and b. During the first twelve hours of simulation, the area averaged convergence in the lower layers is relatively higher in the DB case than that in the AB case. Consistently, area averaged divergence in the upper layers during this period is also higher in the DB case, indicating stronger vertical circulations. During the rest of the simulation period also convergence in the lower layers is slightly stronger in the DB case than in the AB case.

Model prediction of monsoon depression is similar in both AB and the DB cases and location of the predicted depression (not shown) is in agreement with the observations. Since the analyzed rainfall over the location of monsoon depression at the starting time of integration is very small (~ 10 mm d^{-1}), differences of the computed vorticity and divergence associated with the monsoon depression between the AB and the DB cases in the initial conditions are negligible. Also, computed vorticity and divergence maximum associated with the model's monsoon depression in both AB and DB cases are very weak compared to those in the observations. Monsoon depression is not adequately resolved in the initial conditions and this is due to the coarse resolution of the FGGE data. These problems lead to the poor prediction of rainfall associated with the monsoon depression in both the AB and DB cases.

CONCLUSIONS

To study the effects of the initialization procedure on the numerical simulation of monsoon rainfall, two different initial states are specified using adiabatic and diabatic vertical mode initialization schemes. A nested grid model is used to perform simulations for the period 00 UTC 6 July to 8 July. Analyzed rainfall rates for the previous day of starting time are utilized to compute the initial convective heating rates using the Kuo scheme. Results indicate that (a) diabatic initialization helps in predicting higher rainfall rates almost throughout the simulation period, (b) differences in the initialization procedures lead to the prediction of relatively stronger winds and circulation patterns associated with the cumulus convection which in turn increased the evaporation from the surrounding oceanic regions and (c) spinup time re-

mains the same whether initial conditions are prepared using adiabatic or diabatic initialization schemes.

These results also suggest that a proper moisture initialization scheme in conjunction with diabatic initialization scheme may help in improving the model rainfall prediction particularly over the land areas. Also, to improve the model forecast of rainfall associated with the monsoon depression, augmentation of data in the initial conditions is required. Our future work is to incorporate a moisture initialization scheme similar to the one used by Puri and Miller (1990) in to the diabatic initialization scheme and to study its impact on the model forecast and the spinup time.

ACKNOWLEDGEMENTS

This work was supported in part by the Naval Research Laboratory, Washington, D.C. and in part by the Division of International Programs, National Science Foundation under the grant INT-9008926. Computer resources were provided by the North Carolina Supercomputing Center, Research Triangle Park, NC.

REFERENCES

Anthes, R.A., 1977. A cumulus parameterization scheme utilizing a one-dimensional cloud model. Mon. Weather Rev., 105: 207–286.

Davies, H.C., 1976. A lateral boundary formulation for multi-level prediction models. Q. J. R. Meteorol. Soc., 102: 405–418.

Davies, H.C., 1983. Limitations of some common lateral boundary schemes used in regional NWP models. Mon. Weather Rev., 111: 1002–1012.

Krishnamurti, T.N., Cocke, S., Pasch, R. and Low-Nam, S., 1983. Precipitation estimates from rainguage and satellite observations: Summer MONEX. Dep. Meteorol., Florida State Univ., 377 pp.

Kuo, H.L., 1974. Further studies of the parameterization of the influence of cumulus convection on large-scale flow. J. Atmos. Sci., 31: 1232–1240.

Mohanty, U.C., Kasahara, A. and Errico, R., 1986. The impact of diabatic heating on the initialization of divergent circulations in a global forecast model. J. Meteorol. Soc. Jpn., 64(6): 805–817.

Puri, K. and Miller, M.J., 1990. The use of satellite data in the specification of convective heating for diabatic initialization and moisture adjustment in numerical weather prediction models. Mon. Weather Rev., 118: 67–93.

Puri, K., 1987. Some experiments on the use of tropical diabatic heating information for initial state specification. Mon. Weather Rev., 115: 1394–1406.

Turpeinen. O.M., Garand, L., Benoit, R. and Roch, M., 1990. Diabatic initialization of the Canadian regional finite-element (RFE) model using satellite data. Part I: Methodology and application to a winter storm. Mon. Weather Rev., 118: 1381–1395.

Turpeinen, O.M., 1990. Diabatic initialization of the Canadian regional finite-element (RFE) model using satellite data. Part II: Sensitivity to humidity enhancement, Latent-heating profile and rain rates. Mon. Weather Rev., 118: 1396–1407.

Wolcott, S.W. and Warner, T.T., 1981. A moisture analysis procedure utilizing surface and satellite data. Mon. Weather Rev., 113: 1989–1998.